Hopf-bifurcation and Pattern Formation in a host-parasitoid-hyperparasitoid system with Beddington-DeAngelis response

Nitu Kumari*[1], Erik M Bollt[2], Nishith Mohan[1], Sandeep Sharma[1]

[1] *School of Basic Sciences, Indian Institute of Technology Mandi*
Mandi, Himachal Pradesh, 175005, India
[2] *Department of Mathematics and Computer Science,*
Clarkson University, Potsdam, NY, USA

Abstract

We consider a temporal model in which the prey and mid level predator interact via Holling Type IV functional response and mid level predator and top level predator via Beddington Deangelis functional response. We perform local and global stability analysis of the temporal model. We later extend the temporal model spatially and then consider spatially explicit three species predator prey model with Beddington DeAngelis functional response. An extensive bifurcation analysis has been performed and the correlation between the pattern and bifurcation point is studied. Both Turing and non-Turing patterns have been studied. We also observe spatial and temporal chaos in the model. We have investigated the effect of Hopf-bifurcation on Turing and non-Turing pattern formation in the model system.

Keywords: Hopf Bifurcation, Food Chain Model, Pattern Formation

1. Introduction

Patterns in nature and the mechanisms which can generate these patterns is an endless challenge to mathematical modelers . The diversity and beauty of patterns in ecology makes the study even more fascinating. Mathematics provides the natural language for talking about patterns in nature. Since, the ground breaking work of Alan Turing [1] several researchers have contributed in the area. In his seminal work, he explained that activator-inhibitor type chemical reactions can generate interesting patterns due to destabilizing behavior of diffusion, which is counter intuitive to the idea that diffusion always has a strong stabilizing influence. After his work many models in chemistry were studied to verify diffusion as an influencing factor for pattern formation [2–6]. In biology, there is very little knowledge about underlying molecular

*Corresponding author Email :nitu@iitmandi.ac.in

mechanism of skin patterns in animals. Some studies suggest that skin patterns are generated through reaction diffusion systems which are a putative wave of chemical reactions that can generate periodic patterns [7] . Scientists used the spatial models supported by empirical data to explain the localized nature of insect population and to illustrate that dynamic spatial processes regulate the population distribution [8] .The explanation of self regulated pattern formation in nature using reaction diffusion systems was long debated. In a review article, Kondo explained the effective use of reaction diffusion models in experimental biology using the examples from experimental studies [9].

The Beddington DeAngelis functional response is a functional response which describes predator eating response to prey in a similar manner as Holling type II, except that it has an extra term due to mutual interference of predators in the denominator. The simplest form of two dimensional prey predator model with and without diffusion with Beddington DeAngelis functional response has been studied in literature by several authors [10–12]. However, in this work we have focused on spatially extended three species model system with Beddington-DeAngelis functional response because it is more generic and can be applied to understand the dynamics of a wide range of ecological systems. The proposed model describes the temporal evolution due to interaction and movements of hyperparasitoids, parasitoids and hosts population. In literature, researches have tried to understand the interdependence of bifurcation and pattern formation. [12] observed that two dynamical systems having topologically equivalent local dynamics near the Hopf-bifurcation, exhibit a completely different patterning behavior in spatially extended system. An analytical study of diffusive Sel'kov system was done to study Hopf-bifurcation in the model system [13]. Recently there has been much attention focused on Hopf-bifurcation analysis of spatially extended population models, for example [14, 15] and references therein. Recently, Hopf- bifurcation of two dimensional diffusive predator-prey model with Beddington DeAngelis response has been studied to understand global stability of the system [16]. But to the best of our knowledge, the Hopf-bifurcation in three species spatially extended population model with Beddington DeAngelis functional response and its impact on pattern formation has not been studied yet.The objectives of the present study are (i) to investigate the emergence of complex patterns in three species model system as a consequence of spatial distribution of species with Beddington-DeAngelis functional response (ii) to understand the association of Hopf-bifurcation and pattern formation. The organization of remainder of the paper are as follows, in section 2 we discuss formulation of the model system. In section 3, the stability and Hopf-bifurcation analysis of spatially homogeneous case has been discussed. Section 4 discusses the derivation for the conditions for Turing instability in the model system. In section 5, we present spatio temporal pattern formation, Turing pattern formation and Hopf-bifurcation in the model system. We conclude with a discussion of results in section 6.

2. Formulation of the model system

The model system studied in this paper has been developed from the Upadhyay Rai predator prey model [17, 18]. A short introduction to the Upadhyay Rai model is given as follows. Here, $r(t)$ is the generalist top predator predating on $v(t)$ - which is its favorite food, $v(t)$ is the middle specialist predator, predating on $u(t)$, which is the lowest level prey and the favorite food of middle predator. The temporal evolution model for this food chain is given by

$$\begin{aligned} \frac{du}{dt} &= a_1 u\left(1-\frac{u}{K}\right)-\frac{w_0 uv}{(u+D_0)} \\ \frac{dv}{dt} &= -a_2 v+\frac{w_1 uv}{u+D_1}-\frac{w_2 vr}{(v+D_2)} \\ \frac{dr}{dt} &= cr^2-\frac{w_3 r^2}{(v+D_3)} \end{aligned} \tag{2.1}$$

The various parameters [19–21] are described here - a_1 is the rate of self-growth of prey, a_2 is the rate at which middle predator will die out in the absence of its favorite food, $w_i s$ are the maximum value which per capita rate can attain, D_0, D_1, D_2, D_3 are the half saturation constants, K is the carrying capacity of prey u, c is the growth rate of top generalist predator due to sexual reproduction. In this model the top predator r , is predating on v with a predator functional response of *Holling type II.* The model system 2.1 is based on the assumption that species is spatially homogeneously distributed but in nature the species distribution is always spatially in-homogeneous. Therefore, for modeling a realistic food chain scenario, we shall consider the model system with diffusion. When the population distribution changes with location, the predator's rate of feeding upon prey depends on both predator and prey densities. Beddington DeAngelis is one of the predators feeding responses which can arise from spatial mechanism. Therefore, we assume that the population of top predator, r , predating on its favorite food, v, not only allocate time to search for its prey but also spend some time engaging in encounters with other predators of the same population [10]. This results in Beddington DeAngelis functional response of the form $f_1(v,r)=\dfrac{w_2 vr}{(v+br+D_2)}$. This functional response incorporates a predator mutual interference term br in the denominator of Holling type II functional response. The Holling type II functional response of the form $f_2(v,r)=\dfrac{w_2 vr}{(v+D_2)}$ is free from such assumptions[22] during predation. We assume that the top predator's rate of feeding upon prey can be modeled using Beddington DeAngelis functional response instead of Holling type II. Therefore, the system 2.1 can be transformed as follows.

Consider the spatially explicit three species predator prey food chain model system. At any location (x, y) and time t , the interaction of three species populations $u(x, y, t), v(x, y, t)$ and $r(x, y, t)$ can be modeled with the reaction-diffusion equations given by

$$\begin{aligned}
\frac{\partial u}{\partial t} &= a_1 u\left(1-\frac{u}{K}\right) - \frac{w_0 uv}{(u+D_0)} + \delta_1 \Delta u \\
\frac{\partial v}{\partial t} &= -a_2 v + \frac{w_1 uv}{u+D_1} - \frac{w_2 vr}{(v+br+D_2)} + \delta_2 \Delta v \\
\frac{\partial r}{\partial t} &= cr^2 - \frac{w_3 r^2}{(v+D_3)} + \delta_3 \Delta r
\end{aligned} \tag{2.2}$$

$a_1, K, w, D_0, a_2, w_1, D_1, w_2, D_2, c, w_3, D_3$ are positive constants as explained earlier. The new parameter b measures the predator mutual interference. $\delta_1, \delta_2, \delta_3$ are diffusivity constants which signify the spatial movement of prey, middle and top predator populations respectively. The Laplace operator Δ represents , $\Delta = \frac{\partial^2}{\partial x^2}$ in one dimension spatial domain and $\Delta = \left(\frac{\partial^2}{\partial x^2} + \frac{\partial^2}{\partial y^2}\right)$ in two dimensional spatial domain. The problem is based on a bounded domain $\Omega = [0, L_x] \times [0, L_y] \subset R^2$, we consider the following Neumann boundary condition at any time t,

$$(u_x)_{x=0,L_x} = (u_y)_{x=0,L_y} = (v_x)_{x=0,L_x} = (v_y)_{x=0,L_y} = (r_x)_{x=0,L_x} = (r_y)_{x=0,L_y} = 0$$

and positive initial condition.

3. Stability analysis of the temporal system

The proposed model system, without diffusion can be written as follows

$$\begin{aligned}
\frac{du}{dt} &= a_1 u\left(1-\frac{u}{k}\right) - \frac{w_0 uv}{u+D_0} \\
\frac{dv}{dt} &= -a_2 v + \frac{w_1 uv}{u+D_1} - \frac{w_2 vr}{v+br+D_2} \\
\frac{dr}{dt} &= cr^2 - \frac{w_3 r^2}{v+D_3}
\end{aligned} \tag{3.1}$$

above equation's can be written as :

$$\frac{du}{dt} = ug_1, \qquad \frac{dv}{dt} = vg_2, \qquad \frac{dr}{dt} = rg_3. \tag{3.2}$$

where,

$$g_1 = a_1\left(1-\frac{u}{k}\right) - \frac{w_0 v}{u+D_0} \tag{3.3}$$

$$g_2 = -a_2 + \frac{w_1 u}{u+D_1} - \frac{w_2 r}{v+br+D_2} \tag{3.4}$$

$$g_3 = cr - \frac{w_3 r}{v+D_3} \tag{3.5}$$

3.1. Local stability analysis

The system has following equilibrium points :

(i) the trivial equilibrium point $E_0 = (0, 0, 0)$

(ii) the equilibrium point $E_1 = (k, 0, 0)$ exist on the boundary of the first octant

(iii) the planar equilibrium point $E_2 = (\overline{u}, \overline{v}, 0)$ in the $u - v$ plane, where $\overline{u} = \dfrac{a_2 D_1}{a_2 - w_1}$ and $\overline{v} = \dfrac{1}{w_0}\left[a_1\left(1 - \dfrac{\overline{u}}{k}\right)(\overline{u} + D_0)\right]$

The equilibrium point E_2 exist if $a_2 > w_1$ and $k > u$

(iv) The non trivial equilibrium point $E_3 = (u^*, v^*, r^*)$,where
$v^* = \dfrac{w_3}{c} - D_3$,
u^* is a positive solution of the following equation

$$u^{*^2} - k\left(1 - \frac{D_0}{k}\right)u^* - kD_0 + \frac{kw_0}{a_1}v^* = 0$$

and

$$r^* = \frac{(-a_2(u^* + D_1) + w_1 u^*)(v^* + D_2)}{(w_2(u^* + D_1) + ba_2(u^* + D_1) - bw_1 u^*)}$$

Let, the Jacobian matrix at $E_i^{'s}, i = 0, 1, 2, 3$ be $V_i^{'s}, i = 0, 1, 2, 3$. At the trivial equilibrium point E_0, the jacobian matrix V_0, takes the form

$$V_0 = \begin{bmatrix} a_1 & 0 & 0 \\ 0 & -a_2 & 0 \\ 0 & 0 & 0 \end{bmatrix}$$

The eigenvalues of V_0 are a_1, and $-a_2$ which makes E_0 a saddle point.
The Jacobian matrix at E_1 is

$$V_1 = \begin{bmatrix} -a_1 & -\dfrac{kw_0}{k + D_0} & 0 \\ 0 & -a_2 + \dfrac{w_1 k}{k + D_1} & 0 \\ 0 & 0 & 0 \end{bmatrix}$$

From the jacobian matrix V_1, it is found that the equilibrium point E_1 is locally asymptotically stable if $a_2 > \dfrac{w_1 k}{(k + D_1)}$.

The jacobian matrix V_2, at the equilibrium point E_2 is

$$V_2 = \begin{bmatrix} \overline{u}\left(-\frac{a_1}{k}+\frac{w_0\overline{v}}{\overline{u}+D_0}\right) & \overline{u}\left(-\frac{w_0}{\overline{u}+D_0}\right) & 0 \\ \overline{v}\frac{w_1D_1}{(\overline{u}+D_1)^2} & 0 & -\overline{v}\left(\frac{(\overline{v}+D_2)w_2}{(\overline{v}+b\overline{r}+D_2)^2}\right) \\ 0 & 0 & \left(c-\frac{w_3}{(\overline{v}+D_3)}\right) \end{bmatrix}$$

the eigenvalues of the above matrix satisfies the following conditions

$$\lambda_1+\lambda_2 = \overline{u}\left(-\frac{a_1}{k}+\frac{w_0\overline{v}}{\overline{u}+D_0}\right)$$

$$\lambda_1\lambda_2 = -\overline{u}.\overline{v}\left(\frac{w_0}{\overline{u}+D_0}\right)\left(\frac{w_1D_1}{(\overline{u}+D_1)^2}\right)$$

$$\lambda_3 = \left(c-\frac{w_3}{(\overline{v}+D_3)}\right)$$

Hence the system is stable in the $u-v$ plane if $c<\frac{w_3}{(\overline{v}+D_3)}$.

For the non trivial equilibrium point E^*, the jacobian matrix V_3 is given as

$$V_3 = \begin{bmatrix} u^*\left(-\frac{a_1}{k}+\frac{w_0v^*}{(u^*+D_0)^2}\right) & u^*\left(-\frac{w_0}{(u^*+D_0)}\right) & 0 \\ v^*\left(\frac{w_1D_1}{(u^*+D_1)^2}\right) & v^*\left(\frac{w_2r^*}{(v^*+br^*+D_2)^2}\right) & -v^*\left(\frac{w_2(v^*+w_2)}{(v^*+br^*+D_2)^2}\right) \\ 0 & r^*\left(\frac{w_3r^*}{(v^*+D_3)^2}\right) & r^*\left(c-\frac{w_3}{(v^*+w_3)}\right) \end{bmatrix}$$

The characteristic equation of the above matrix is

$$\lambda^3+A_1\lambda^2+A_2\lambda+A_3=0 \tag{3.6}$$

where,

$$A_1 = \left[u^*\left(-\frac{a_1}{k}+\frac{w_0v^*}{(u^*+D_0)^2}\right)+v^*\left(\frac{w_2r^*}{(v^*+br^*+D_2)^2}\right)+r^*\left(c-\frac{w_3}{(v^*+w_3)}\right)\right]$$

$$\begin{aligned}A_2 =& u^*v^*\left(-\frac{a_1}{k}+\frac{w_0v^*}{(u^*+D_0)^2}\right)\left(\frac{w_2r^*}{(v^*+br^*+D_2)^2}\right)+u^*r^*\left(-\frac{a_1}{k}+\frac{w_0v^*}{(u^*+D_0)^2}\right)\left(c-\frac{w_3}{(v^*+w_3)}\right)\\ &+v^*r^*\left(\frac{w_2r^*}{(v^*+br^*+D_2)^2}\right)\left(c-\frac{w_3}{(v^*+w_3)}\right)+v^*r^*\left(\frac{w_3r^*}{(v^*+D_3)^2}\right)\left(\frac{w_2(v^*+w_2)}{(v^*+br^*+D_2)^2}\right)\\ &+u^*v^*\left(\frac{w_0}{(u^*+D_0)}\right)\left(\frac{w_1D_1}{(u^*+D_1)^2}\right)\\ A_3 =& -\left[u^*v^*r^*\left(-\frac{a_1}{k}+\frac{w_0v^*}{(u^*+D_0)^2}\right)\left(\frac{w_2r^*}{(v^*+br^*+D_2)^2}\right)\left(c-\frac{w_3}{(v^*+w_3)}\right)\right]\\ &-\left[u^*v^*r^*\left(-\frac{a_1}{k}+\frac{w_0v^*}{(u^*+D_0)^2}\right)\left(\frac{w_2(v^*+w_2)}{(v^*+br^*+D_2)^2}\right)\left(\frac{w_3r^*}{(v^*+D_3)^2}\right)\right]\\ &-\left[u^*v^*r^*\left(-\frac{w_0}{(u^*+D_0)}\right)\left(\frac{w_1D_1}{(u^*+D_1)^2}\right)\left(c-\frac{w_3}{(v^*+w_3)}\right)\right]\end{aligned}$$

Applying Routh-Hurwitz criteria to equation 3.6 gives the following theorem :

Theorem 1 The non-trivial equilibrium point E_3 is locally asymptotically provided $A_i > 0, i = 1, 2, 3$ and $A_1A_2 - A_3 > 0$

Through the conditions derived earlier for different equilibrium points and by calculations the above criteria has been proved.

3.2. Global stability analysis

We here state the theorem for global existence of the non-trivial equilibrium point E_3.

Theorem 2 The non trivial equilibrium point E_3 is globally asymptotically stable under the following condition :

$$c < \frac{w_3}{\gamma}(v^*+D_3) \text{ and } \left(\frac{a_1}{k}+\frac{w_0v^*}{\alpha}\right)(u-u^*)^2 > \frac{\beta_1w_2r^*}{\beta_2w_1D_1}(v-v^*)^2 \tag{3.7}$$

Proof We use Lyapunov direct method to prove global existence of the non trivial equilibrium point. For that purpose we consider the following Lyapunov function

$$V = C_1\left[u-u^*-u^*ln\left(\frac{u}{u^*}\right)\right]+C_2\left[v-v^*-v^*ln\left(\frac{v}{v^*}\right)\right]+C_3\left[r-r^*-r^*ln\left(\frac{r}{r^*}\right)\right],$$

where, $C_i, i = 1, 2, 3$ are arbitrary constants to be evaluated.

i.e. $V = V_1 + V_2 + V_3$, where,

$$V_1 = C_1\left[u-u^*-u^*ln\left(\frac{u}{u^*}\right)\right], V_2 = C_2\left[v-v^*-v^*ln\left(\frac{v}{v^*}\right)\right]; V_3 = C_3\left[r-r^*-r^*ln\left(\frac{r}{r^*}\right)\right]$$

The derivative of V with respect to the time along the solution of the model system 3.1is

$$\frac{dV}{dt} = \frac{dV_1}{dt} + \frac{dV_2}{dt} + \frac{dV_3}{dt} \tag{3.8}$$

Here,

$$\frac{dV_1}{dt} = C_1\left(\frac{u-u^*}{u}\right)\frac{du}{dt}$$
$$\frac{dV_1}{dt} = C_1\left(\frac{u-u^*}{u}\right)\left(a_1 u\left(1-\frac{u}{k}\right) - \frac{w_0 uv}{u+D_0}\right)$$

On, simplification we obtain,

$$\frac{dV_1}{dt} = -C_1\left(\frac{a_1}{k} + \frac{w_0 v^*}{\alpha}\right)(u-u^*)^2 - \frac{C_1 w_0}{\alpha}(u^*+D_0)(v-v^*)(u-u^*) \tag{3.9}$$

where $\alpha = (u+D_0)(u^*+D_0)$.

Similarly, we can obtain the following

$$\frac{dV_2}{dt} = \left(\frac{C_2 w_1 D_1}{\beta_1}\right)(u-u^*)(v-v^*) - \left(\frac{C_2 w_2}{\beta_2}\right)(v^*+D_2)(r-r^*)(v-v^*) + \left(\frac{C_2 w_2 r^*}{\beta_2}\right)(v-v^*)^2 \tag{3.10}$$

where $\beta_1 = (u-u^*)(u^*+D_1)$ and $\beta_2 = (v+br+D_2)(v^*+br^*+D_2)$

and

$$\frac{dV_3}{dt} = C_3\left(c - \frac{w_3 v^*}{\gamma} - \frac{D_3 w_3}{\gamma}\right)(r-r^*)^2 + \left(\frac{C_3 w_3 r^*}{\gamma}\right)(v-v^*)(r-r^*) \tag{3.11}$$

where, $\gamma = (v+D_3)(v^*+D_3)$

From above equations, we obtain,

$$\begin{aligned}\frac{dV}{dt} =& C_1\left(\frac{a_1}{k} + \frac{w_0 v^*}{\alpha}\right)(u-u^*)^2 - C_1\frac{w_0}{\alpha}\left(u^*-D_0\right)(v-v^*)(u-u^*)\\ &+\left(\frac{C_2 w_1 D_1}{\beta_1}\right)(u-u^*)(v-v^*) - \left(\frac{C_2 w_2}{\beta_2}\right)(v^*+D_2)(r-r^*)(v-v^*)\\ &+\left(\frac{C_2 w_2 r^*}{\beta_2}\right)(v-v^*)^2 + C_3\left(c - \frac{w_3 v^*}{\gamma} - \frac{D_3 w_3}{\gamma}\right)(r-r^*)^2\\ &+\left(\frac{C_3 w_3 r^*}{\gamma}\right)(v-v^*)(r-r^*)\end{aligned}$$

Choosing,

$$C_1 = 1, \quad C_2 = \frac{\beta_1 w_0(u^*+D_0)}{\alpha w_1 D_1} \quad \text{and} \quad C_3 = \frac{C_2 \gamma w_2 (v^*+D_2)}{\beta_2 w_3 r^*}$$

we obtain the following,

$$\frac{dV}{dt} = -\left(\frac{a_1}{k} + \frac{w_0 v^*}{\alpha}\right)(u-u^*)^2 + \frac{\beta_1 w_2 r^*}{\beta_2 w_1 D_1}(v-v^*)^2 + \frac{\gamma\beta_1}{w_1 w_3 r^* D_1}\left(c - \frac{w_3}{\gamma}v^* - \frac{D_3 w_3}{\gamma}\right)(r-r^*)^2$$

Now, $\dfrac{dV}{dt}$ is clearly negative definite under condition 3.7, stated in the theorem. Hence the nontrivial equilibrium point E_3 is globally asymptotically stable.

4. Existence of Hopf-bifurcation

We will now prove the existence of Hopf-bifurcation in the system by considering a_1 - the rate of self growth of prey as the bifurcation parameter.

If there exist $a_1 = a_{1_0}$ then the necessary and sufficient and sufficient conditions for the existence of the Hopf-bifurcation are

(i) $A_i(a_{1_0}) > 0, i = 1, 2, 3$

(ii) $A_1(a_{1_0})A_2(a_{1_0}) - A_3(a_{1_0}) = 0$ and

(iii) $\mathrm{Re}\left(\dfrac{du_i}{dr}\right) \neq 0, i = 1, 2, 3$, where u_is is the real part of the eigenvalues of the characteristic equation of the form $\lambda_i = p_i + iq_i$

Now, we verify the condition (iii) for the existence of Hopf-bifurcation. Put $\lambda_i = p_i + iq_i$ in (14), we get,

$$(p + iq)^3 + A_1(p + iq)^2 + A_3(p + iq) + A_3 = 0 \tag{4.1}$$

on separating the real and imaginary parts and eliminating q between them, we get,

$$8p^3 + 8A_1p^2 + 2(A_1^2 + A_2)p + A_1A_2 - A_3 = 0 \tag{4.2}$$

Now we have $p(a_{1_0}) = 0$ as $A_1(a_{1_0})A_1(a_{1_0}) - A_1(a_{1_0}) = 0$ and $a_1 = a_{1_0}$ is the only positive root of $A_1(a_{1_0})A_2(a_1) - A_3(a_{1-0}) = 0$, and the discriminant of $8p^2 + 8A_1p + 2(A_1^2 + A_2) = 0$ is $-64A_2 < 0$. On differentiating (21) with respect to a_1, we get,

$$(24p^2 + 16A_1p + 2(A_1^2 + A_2))\frac{dp}{da_1} + (8p^2 + 4A_1p)\frac{dA_1}{da_1} + 2p\frac{dA_2}{da_1} + \frac{d}{da_1}(A_1A_2 - A_3) = 0 \tag{4.3}$$

Now at $a_1 = a_{1_0}$, $p(a_{1_0}) = 0$, we obtain

$$\left(\frac{dp}{da_1}\right)_{a_1=a_{1_0}} = \frac{-\frac{d}{da_1}(A_1A_2 - A_3)}{2(A_1^2 + A_2)} \neq 0 \tag{4.4}$$

which ensures that the above system has Hopf-bifurcation.

5. Stability Analysis of Spatially Extended Model System

In this section, we will study the dynamical behavior of the model with diffusion. For that purpose we will first analyze the model in one dimensional spatial domain $[0, \Omega]$. Diffusion is introduced as the principal mechanism of motion. The model takes the form

$$\begin{aligned}
\frac{\partial u}{\partial t} &= a_1u\left(1 - \frac{u}{k}\right) - \frac{w_0uv}{u + D_0} + \delta_1\frac{\partial^2 u}{\partial x^2}\\
\frac{\partial v}{\partial t} &= -a_2v + \frac{w_1uv}{u + D_1} - \frac{w_2vr}{v + br + D_2} + \delta_2\frac{\partial^2 v}{\partial x^2}\\
\frac{\partial r}{\partial t} &= cr^2 - \frac{w_3r^2}{v + D_3} + \delta_3\frac{\partial^2 r}{\partial x^2}
\end{aligned} \tag{5.1}$$

The above system will be studied with positive initial conditions given by

$$u(x,0) \geq 0; v(x,0) \geq 0; r(x,0) \geq 0.$$

and boundary conditions:

$$\frac{\partial u}{\partial x}\Big|_{x=0,\Omega} = \frac{\partial v}{\partial x}\Big|_{x=0,\Omega} = \frac{\partial r}{\partial x}\Big|_{x=0,\Omega} = 0.$$

For the above model system, we consider eigenfunctions of the form

$$\begin{pmatrix} u \\ v \\ r \end{pmatrix} = \begin{pmatrix} a \\ b \\ c \end{pmatrix} \exp(\lambda t + ikx)$$

Hence, we have,

$$\begin{aligned} u &= a \exp(\lambda t + ikx), \\ v &= b \exp(\lambda t + ikx), \\ r &= c \exp(\lambda t + ikx) \end{aligned} \tag{5.2}$$

where, λ is wavelength and k is the wave number.

Thus from the above expression of u, v and r, we have,

$$\frac{\partial^2 u}{\partial x^2} = -k^2 a \exp(\lambda t + ikx) \quad \text{or} \quad \frac{\partial^2 u}{\partial x^2} = -k^2 u, \quad \text{similarly} \quad \frac{\partial^2 v}{\partial x^2} = -k^2 v \quad \text{and} \quad \frac{\partial^2 r}{\partial x^2} = -k^2 r.$$

Hence, the above model becomes

$$\begin{aligned} \frac{\partial u}{\partial t} &= a_1 u \left(1 - \frac{u}{k}\right) - \frac{w_0 uv}{u + D_0} - \delta_1 k^2 u \\ \frac{\partial v}{\partial t} &= -a_2 v + \frac{w_1 uv}{u + D_1} - \frac{w_2 vr}{v + br + D_2} - \delta_2 k^2 v \\ \frac{\partial r}{\partial t} &= cr^2 - \frac{w_3 r^2}{v + D_3} - \delta_3 k^2 r \end{aligned} \tag{5.3}$$

5.1. Local stability Analysis of Model in one-dimensional spatial domain

To perform the local stability analysis at the equilibrium points $E_i, i = 0, 1, 2, 3,$ we first obtain the jacobian matrix of the system 5.3at each of the equilibrium point. The jacobian matrix at E_0 is given by

$$V_0 = \begin{bmatrix} a_1 - \delta_1 k^2 & 0 & 0 \\ 0 & -a_2 - \delta_2 k^2 & 0 \\ 0 & 0 & -\delta_3 k^2 \end{bmatrix}$$

The eigenvalues of V_0 are $a_1 - \delta_1 k^2$, $-a_2 - \delta_2 k^2$ and $-\delta_3 k^2$. Thus the equilibrium point E_0 is

(i) stable if $a_1 < \delta_1 k^2$,

(ii) saddle if $a_1 > \delta_1 k^2$.

The Jacobian matrix at E_1 is given by

$$V_1 = \begin{bmatrix} -a_1 - \delta_1 k^2 & -\dfrac{kw_0}{k+D_0} & 0 \\ 0 & -a_2 + \dfrac{w_1 k}{k+D_1} - \delta_2 k^2 & 0 \\ 0 & 0 & -\delta_3 k^2 \end{bmatrix}$$

From V_1, we can conclude that equilibrium point E_1 is

(i) saddle if $\dfrac{w_1 k}{k+D_1} > (a_2 + \delta_2 k^2)$,

(ii) stable if $\dfrac{w_1 k}{k+D_1} < (a_2 + \delta_2 k^2)$.

The jacobian matrix at E_2 is

$$V_2 = \begin{bmatrix} \overline{u}\left(-\dfrac{a_1}{k} + \dfrac{w_0\overline{v}}{\overline{u}+D_0}\right) - \delta_1 k^2 & \overline{u}\left(-\dfrac{w_0}{\overline{u}+D_0}\right) & 0 \\ \overline{v}\frac{w_1 D_1}{(\overline{u}+D_1)^2} & -\delta_2 k^2 & -\overline{v}\left(\dfrac{(\overline{v}+D_2)w_2}{(\overline{v}+b\overline{r}+D_2)^2}\right) \\ 0 & 0 & \left(c - \dfrac{w_3}{(\overline{v}+D_3)}\right) - \delta_3 k^2 \end{bmatrix}$$

The eigenvalues of the above jacobian matrix satisfies the following conditions

$$\begin{aligned} \lambda_1 + \lambda_2 &= \overline{u}\left(-\frac{a_1}{k} + \frac{w_0 v_1}{\overline{u}+D_0}\right) - (\delta_1+\delta_2)K^2, \\ \lambda_1\lambda_2 &= \left[\left\{\overline{u}\left(\frac{a_1}{k} + \frac{w_0\overline{v}}{\overline{u}+D_0}\right) - \delta_1 k^2\right\}\delta_2 k^2\right] - \overline{uv}\left(\frac{w_0}{\overline{u}+D_0}\right)\left(\frac{w_1 D_1}{(\overline{u}+D_1)^2}\right) - (\delta_1+\delta_2)K^2 \\ \lambda_3 &= \left(c - \frac{w_3}{(\overline{v}+D_3)}\right) - \delta_3 k^2 \end{aligned}$$

Therefore, the equilibrium point E_2 is stable under the following conditions

(i) $c < \left(\dfrac{w_3}{\overline{v}+D_3}\right) + \delta_3 k^2$

(ii) $\overline{u}\left(-\dfrac{a_1}{k} + \dfrac{w_0\overline{v}}{\overline{u}+D_0} - \delta k^2\right)(\delta_2 k^2) > \overline{uv}\left(\dfrac{w_0}{\overline{u}+D_0}\right)\left(\dfrac{w_1 D_1}{(\overline{u}+D_1)^2}\right) + (\delta_1+\delta_2)K^2$

(iii) $\overline{u}\dfrac{a_1}{k} + (\delta_1+\delta_2)k^2 > \dfrac{w_0 u\overline{u}}{\overline{u}+D_0}$

The jacobian matrix at non trivial equilibrium point is given by

$$V_3 = \begin{bmatrix} u^*\left(-\frac{a_1}{k} + \frac{w_0 v^*}{(u^*+D_0)^2}\right) - \delta_1 k^2 & u^*\left(-\frac{w_0}{(u^*+D_0)}\right) & 0 \\ v^*\left(\frac{w_1 D_1}{(u^*+D_1)^2}\right) & v^*\left(\frac{w_2 r^*}{(v^*+br^*+D_2)^2}\right) - \delta_2 k^2 & -v^*\left(\frac{w_2(v^*+w_2)}{(v^*+br^*+D_2)^2}\right) \\ 0 & r^*\left(\frac{w_3 r^*}{(v^*+D_3)^2}\right) & r^*\left(c - \frac{w_3}{(v^*+w_3)}\right) - \delta_3 k^2 \end{bmatrix}$$

The characteristic equation of the jacobian matrix V_3 is,

$$\lambda^3 + A_1\lambda^2 + A_2\lambda + A_3 = 0$$

where,

$$\begin{aligned}
A_1 &= \Big[u^*\left(-\frac{a_1}{k} + \frac{w_0 v^*}{(u^*+D_0)^2}\right) - \delta_1 k^2 + v^*\left(\frac{w_2 r^*}{(v^*+br^*+D_2)^2}\right) - \delta_2 k^2 \\
&\quad + r^*\left(c - \frac{w_3}{(v^*+w_3)}\right) - \delta_3 k^2\Big] \\
A_2 &= \left(u^*\left(-\frac{a_1}{k} + \frac{w_0 v^*}{(u^*+D_0)^2}\right) - \delta_1 k^2\right)\left(v^*\left(\frac{w_2 r^*}{(v^*+br^*+D_2)^2}\right) - \delta_2 k^2\right) \\
&\quad + \left(u^*\left(-\frac{a_1}{k} + \frac{w_0 v^*}{(u^*+D_0)^2}\right) - \delta_1 k^2\right)\left(r^*\left(c - \frac{w_3}{(v^*+w_3)}\right) - \delta_3 k^2\right) \\
&\quad + \left(v^*\left(\frac{w_2 r^*}{(v^*+br^*+D_2)^2}\right) - \delta_2 k^2\right)\left(r^*\left(c - \frac{w_3}{(v^*+w_3)}\right) - \delta_3 k^2\right) \\
&\quad + \left(u^*\left(-\frac{w_0}{(u^*+D_0)}\right)\right)\left(v^*\left(\frac{w_1 D_1}{(u^*+D_1)^2}\right)\right) \\
&\quad - \left(v^*\left(\frac{w_2(v^*+w_2)}{(v^*+br^*+D_2)^2}\right)\right)\left(r^*\left(\frac{w_3 r^*}{(v^*+D_3)^2}\right)\right) \\
A_3 &= \left[\left(u^*\left(-\frac{a_1}{k} + \frac{w_0 v^*}{(u^*+D_0)^2}\right) - \delta_1 k^2\right)\left(v^*\left(\frac{w_2(v^*+w_2)}{(v^*+br^*+D_2)^2}\right)\right)\left(r^*\left(\frac{w_3 r^*}{(v^*+D_3)^2}\right)\right)\right] \\
&\quad + \left[\left(u^*\left(-\frac{w_0}{(u^*+D_0)}\right)\right)\left(v^*\left(\frac{w_1 D_1}{(u^*+D_1)^2}\right)\right)\left(r^*\left(c - \frac{w_3}{(v^*+w_3)}\right) - \delta_3 k^2\right)\right] \\
&\quad - \left(u^*\left(-\frac{a_1}{k} + \frac{w_0 v^*}{(u^*+D_0)^2}\right) - \delta_1 k^2\right)\left(v^*\left(\frac{w_2 r^*}{(v^*+br^*+D_2)^2}\right) - \delta_2 k^2\right)\left(r^*\left(c - \frac{w_3}{(v^*+w_3)}\right) - \delta_3 k^2\right)
\end{aligned}$$

By Routh-Hurwitz criteria of local stability, E_3 is locally stable if $A_i > 0, i = 1, 2, 3$ and $A_1A_2 - A_3 > 0$.

5.2. Global stability analysis of one dimensional diffusion model

The global stability of one dimensional diffusion model has been established by the following theorem

Theorem 3: (1) If E^* is globally asymptotically stable for model without diffusion then it is also globally asymptotically stable for our diffusion model.

(2) If non trivial equilibrium E^* is unstable for model without diffusion then the diffusion

model can be made globally asymptotically stable by increasing the diffusion coefficients to a sufficiently large value.

Proof: We consider the following functional
$V_1 = \int_0^{\Omega} V(u,v,r)dx$
on differentiating with respect to time, we get

$$\frac{dV_1}{dt} = \int_0^{\Omega} \left[\left(\frac{\partial V}{\partial u}\right)\left(\frac{\partial u}{\partial t}\right) + \left(\frac{\partial V}{\partial v}\right)\left(\frac{\partial v}{\partial t}\right) + \left(\frac{\partial V}{\partial r}\right)\left(\frac{\partial r}{\partial t}\right) \right] dx$$

on putting the values of $\frac{\partial u}{\partial t}$, $\frac{\partial v}{\partial t}$ and $\frac{\partial r}{\partial t}$ in the above expression, we obtain

$$\begin{aligned} \frac{dV_1}{dt} &= \int_0^{\Omega} \left[\left(\frac{\partial V}{\partial u}\right)\left(a_1 u(1-\frac{u}{k}) - \frac{w_0 uv}{u+D_0} + \delta_1 \left(\frac{\partial^2 u}{\partial x^2}\right)\right)\right] dx \\ &+ \int_0^{\Omega} \left[\left(\frac{\partial V}{\partial v}\right)\left(-a_2 v + \frac{w_1 uv}{u+D_1} - \frac{w_2 vr}{v+br+D_2} + \delta_2 \frac{\partial^2 v}{\partial x^2}\right)\right] dx \\ &+ \int_0^{\Omega} \left[\left(\frac{\partial V}{\partial r}\right)\left(cr^2 - \frac{w_3 r^2}{v+D_3} + \delta_3 \frac{\partial^2 r}{\partial x^2}\right)\right] dx \end{aligned}$$

Or

$$\begin{aligned} \frac{dV_1}{dt} &= \int_0^{\Omega} (\frac{dV}{dt})dx - \delta_1 \int_0^{\Omega} \left(\frac{\partial^2 V}{\partial^2 u^2}\right)\left(\frac{\partial u}{\partial x}\right)^2 dx - \delta_2 \int_0^{\Omega} \left(\frac{\partial^2 V}{\partial^2 v^2}\right)\left(\frac{\partial v}{\partial x}\right)^2 dx \\ &- \delta_3 \int_0^{\Omega} \left(\frac{\partial^2 V}{\partial^2 r^2}\right)\left(\frac{\partial r}{\partial x}\right)^2 dx \end{aligned}$$

On putting the values of $\left(\frac{\partial^2 V}{\partial^2 u^2}\right)$, $\left(\frac{\partial^2 V}{\partial^2 v^2}\right)$ and $\left(\frac{\partial^2 V}{\partial^2 r^2}\right)$, we get

$$\frac{dV_1}{dt} = \int_0^{\Omega} \left(\frac{dV}{dt}\right) dx - \delta_1 \int_0^{\Omega} \frac{u^*}{u^2}\left(\frac{\partial u}{\partial x}\right)^2 dx - \delta_2 \int_0^{\Omega} \frac{v^*}{v^2}\left(\frac{\partial v}{\partial x}\right)^2 dx - \delta_3 \int_0^{\Omega} \frac{r^*}{r^2}\left(\frac{\partial r}{\partial x}\right)^2 dx$$

Therefore when $\frac{dV}{dt}$ is negative, the system is globally asymptotically stable.
If $\frac{dV_1}{dt}$ is not negative, then we can make the system globally asymptotically stable by increasing the diffusion coefficient sufficiently large. Hence the theorem.

5.3. Local stability Analysis of Model in two dimensional spatial domain

Here we consider the model system given in 2.2 in two dimensional spatial domain.
We consider the solution of the following form

$$\begin{pmatrix} u \\ v \\ r \end{pmatrix} = \begin{pmatrix} a \\ b \\ c \end{pmatrix} \exp(\lambda t + i(k_x x + k_y y))$$

where $u = a\ \exp(\lambda t + i(k_x x + k_y y))$, $v = b\ \exp(\lambda t + i(k_x x + k_y y))$ and $r = c\ \exp(\lambda t + i(k_x x + k_y y))$ where, λ is frequency and k_x and k_y are the components of wave number k along x and y directions.

Substituting these values in the model system, we can obtain

$\nabla^2 u = -k^2 u$, $\nabla^2 v = -k^2 v$ and $\nabla^2 r = -k^2 r$, where, $k^2 = k_x^2 + k_y^2$. Putting the above values in the model,we obtain the new model as follows

$$\frac{\partial u}{\partial t} = a_1 u\left(1 - \frac{u}{k}\right) - \frac{w_0 uv}{u + D_0} - \delta_1 k^2 u \tag{5.4}$$

$$\frac{\partial v}{\partial t} = -a_2 v + \frac{w_1 uv}{u + D_1} - \frac{w_2 vr}{v + br + D_2} - \delta_2 k^2 v \tag{5.5}$$

$$\frac{\partial r}{\partial t} = cr^2 - \frac{w_3 r^2}{v + D_3} - \delta_3 k^2 r \tag{5.6}$$

As the model with two dimensional diffusion is similar to that of one dimensional diffusion, therefore the results of local stability of two dimensional diffusion model are equally applicable to for the two dimensional diffusion model.

5.4. Global stability Analysis of two dimensional diffusion model

The following theorem the global stability of two dimensional diffusion model

Theorem 4 (1) If E^* is globally asymptotically stable for model without diffusion then it is also globally asymptotically stable for our diffusion model.

(2) If non trivial equilibrium E^* is unstable for model without diffusion then the diffusion model can be made globally asymptotically stable by increasing the diffusion coefficients to a sufficiently large value.

Proof: To prove the above result, we consider the following functional

$$V_2(t) = \iint_\Omega V(u, v, r)dA$$

Differentiating the above functional with respect to time and along the solution of the two dimensional diffusion model, we obtain

$$V_2'(t) = \iint_\Omega \left[\left(\frac{\partial V}{\partial u}\right)\left(\frac{\partial u}{\partial t}\right) + \left(\frac{\partial V}{\partial v}\right)\left(\frac{\partial v}{\partial t}\right) + \left(\frac{\partial V}{\partial r}\right)\left(\frac{\partial r}{\partial t}\right)\right] dA$$

on putting the values of $\frac{\partial u}{\partial t}$, $\frac{\partial v}{\partial t}$ and $\frac{\partial r}{\partial t}$ in the above expression, we obtain

$$V_2^{'}(t) = \iint\limits_{\Omega} \left[\left(\frac{\partial V}{\partial S}\right)\left(a_1 u\left(1-\frac{u}{k}\right) - \frac{w_0 uv}{u+D_0} + \delta_1 \bigtriangleup u\right)\right] dA +$$
$$\iint\limits_{\Omega} \left[\left(\frac{\partial V}{\partial I}\right)(-a_2 v + \frac{w_1 uv}{u+D_1} - \frac{w_2 vr}{v+br+D_2} + \delta_2 \bigtriangleup v\right] dA +$$
$$\iint\limits_{\Omega} \left[\left(\frac{\partial V}{\partial R}\right)(cr^2 - \frac{w_3 r^2}{v+D_3} + \delta_3 \bigtriangleup r\right] dA$$

We can write the above expression as a sum of two integrals as follows

$$\frac{dV_2}{dt} = I_1 + I_2$$

Where,

$$I_1 = \iint\limits_{\Omega} \left[\left(\frac{dV}{dt}\right)\right] dA$$
$$I_2 = \iint\limits_{\Omega} \left[\delta_1\left(\frac{\partial V}{\partial u}\right) \bigtriangleup uu + \delta_2\left(\frac{\partial V}{\partial v}\right) \bigtriangleup uv + \delta_3\left(\frac{\partial V}{\partial r}\right) \bigtriangleup ur\right] dA$$

Now, according to the Green's identity in the plane, we have the following result

$$\iint\limits_{\Omega} F \bigtriangleup uQ dA = \int_{\partial\Omega} F\frac{\partial Q}{\partial n} ds - \iint\limits_{\Omega} (\bigtriangledown F. \bigtriangledown Q)\, dA$$
$$\delta_1 \iint\limits_{\Omega} \left(\left(\frac{\partial V}{\partial u}\right) \bigtriangleup uu\right) dA = -\delta_1 \iint\limits_{\Omega} \left(\frac{\partial^2 V}{\partial u^2}\right)\left(\left(\frac{\partial u}{\partial x}\right)^2 + \left(\frac{\partial u}{\partial y}\right)^2\right) dA$$
$$\leq 0$$

similarly,

$$\delta_2 \iint\limits_{\Omega} \left(\left(\frac{\partial V}{\partial v}\right) \bigtriangleup v\right) dA = -\delta_2 \iint\limits_{\Omega} \left(\frac{\partial^2 V}{\partial v^2}\right)\left(\left(\frac{\partial v}{\partial x}\right)^2 + \left(\frac{\partial v}{\partial y}\right)^2\right) dA$$
$$\leq 0$$

and

$$\delta_3 \iint\limits_{\Omega} \left(\left(\frac{\partial V}{\partial r}\right) \bigtriangleup r\right) dA = -\delta_3 \iint\limits_{\Omega} \left(\frac{\partial^2 V}{\partial r^2}\right)\left(\left(\frac{\partial r}{\partial x}\right)^2 + \left(\frac{\partial r}{\partial y}\right)^2\right) dA$$
$$\leq 0$$

Thus, it is clear that $I_2 \leq 0$ and hence $\dfrac{dV_2}{dt} < 0$ if $I_1 \leq 0$.

Therefore, we can conclude that, if E^* is stable in the absence of diffusion then it will remain globally asymptotically stable in the presence of diffusion.

5.5. Diffusion Driven Instability

In this section, we will study in detail the local dynamics and stability conditions of the spatially explicit case of the model system in a two dimensional spatial domain. We also obtain here the conditions for the diffusion driven instability to occur by perturbing the homogeneous steady state solution. The stability analysis of model system 2.2 is carried out with positive initial conditions and zero flux boundary conditions given by

$$r(x,y,0) \geq 0, \quad r(x,y,0) \geq 0, \quad r(x,y,0) \geq 0$$

$$(u_x)_{x=0,L_x} = (u_y)_{x=0,L_y} = (v_x)_{x=0,L_x} = (v_y)_{x=0,L_y} = (r_x)_{x=0,L_x} = (r_y)_{x=0,L_y} = 0$$

$$\text{where} \quad 0 < x < L_x \quad \text{and} \quad 0 < y < L_y$$

.

For the linear stability analysis of spatially extended model (4)-(6), steady state is perturbed with the following two dimensional spatio-temporal perturbation of the form

$$u = u^* + a\exp(\lambda_k t + i(k_x x + k_y y)) = u^* + u_1 \tag{5.7}$$

$$v = v^* + b\exp(\lambda_k t + i(k_x x + k_y y)) = v^* + v_1 \tag{5.8}$$

$$r = r^* + c\exp(\lambda_k t + i(k_x x + k_y y)) = r^* + r_1 \tag{5.9}$$

where a, b and c are sufficiently small constants, k_x and k_y are the components of wave number k along x and y directions respectively and λ_k is the wavelength. The system is linearized about the equilibrium point $E(u^*, v^*, r^*)$.
The characteristic equation of the linearized version of the spatial model system 2.2 is given by

$$(J_{uvr} - \lambda_k I_3)\begin{bmatrix} a \\ b \\ c \end{bmatrix} = 0 \tag{5.10}$$

with

$$J_{uvr} = \begin{bmatrix} a_{11} - \delta_1 k^2 & a_{12} & 0 \\ a_{21} & a_{22} - \delta_2 k^2 & a_{23} \\ 0 & a_{32} & -\delta_3 k^2 \end{bmatrix}$$

where k is the wave number given by $k^2 = k_x^2 + k_y^2$ and I_3 is a 3×3 identity matrix in which,

$$\begin{aligned}
a_{11} &= u^* \left(-\frac{a_1}{k} + \frac{w_0 v^*}{(u^* + D_0)^2}\right) & a_{12} &= \frac{-w_0 u^*}{(u^* + D_0)} \\
a_{21} &= \frac{w_1 D_1 v^*}{(u^* + D_1)^2}, & a_{22} &= \frac{w_2 r^* (v^* + 2(D_2 + br^*))}{(v^* + br^* + D_2)^2}, \\
a_{23} &= \frac{-w_2 v^* (v^* + D_2)}{(v^* + br^* + D_2)^2}, & a_{32} &= \frac{c^2 r^{*2}}{w_3}
\end{aligned}$$

Our interest is the stability properties of the attracting interior equilibrium point E , which will lead to the conditions for diffusion driven instability. From 5.10, we get the characteristic equation of the form

$$\begin{aligned}
\det(J_{uvr} - \lambda_k I_3) =& \lambda_k^3 - \operatorname{tr}(J_{uvr})\lambda_k^2 + \lambda_k[(\delta_1\delta_2 + \delta_2\delta_3 + \delta_3\delta_1)k^4 - (a_{11}(\delta_2 + \delta_3) + a_{22}(\delta_1 + \delta_3)k^2) \\
&+ a_{11}a_{22} - a_{23}a_{32} - a_{12}a_{21}] - \det(J_{uvr}) = 0
\end{aligned} \tag{5.11}$$

The characteristic equation can be written as

$$\det(J_{uvr} - \lambda_k I_3) = \lambda_k^3 + \rho_1 \lambda_k^2 + \rho_2 \lambda_k + \rho_3 \tag{5.12}$$

where

$$\begin{aligned}
\rho_1 =& -\operatorname{tr}(J_{uvr}) \\
\rho_2 =& (\delta_1\delta_2 + \delta_2\delta_3 + \delta_3\delta_1)k^4 - (a_{11}(\delta_2 + \delta_3) + a_{22}(\delta_1 + \delta_3)k^2) + a_{11}a_{22} - a_{23}a_{32} - a_{12}a_{21}] \\
\rho_3 =& -\det(J_{uvr})
\end{aligned} \tag{5.13}$$

An application of the Routh-Hurwitz criteria gives the following theorem immediately.

Theorem 5 The interior equilibrium point $E_3(u^*, v^*, r^*)$ is locally asymptotically stable in the presence of diffusion if and only if the following three conditions are satisfied:

$$u^* \left(-\frac{a_1}{k} + \frac{w_0 v^*}{(u^* + D_0)^2}\right) + \frac{w_2 r^* (v^* + 2(D_2 + br^*))}{(v^* + br^* + D_2)^2} < (\delta_1 + \delta_2 + \delta_3)k^2, \tag{5.14}$$

$$\begin{aligned}
& u^* \left(-\frac{a_1}{k} + \frac{w_0 v^*}{(u^* + D_0)^2}\right)\delta_2 + \frac{w_2 r^* (v^* + 2(D_2 + br^*))}{(v^* + br^* + D_2)^2}\delta_1 - \frac{w_0 w_1 D_1 u^* v^*}{k^2 (u^* + D_0)(u^* + D_1)^2} \\
& - \frac{w_2 u^* r^*}{k^2}\left(-\frac{a_1}{k} + \frac{w_0 v^*}{(u^* + D_0)^2}\right)\left(\frac{(v^* + 2(D_2 + br^*))}{(v^* + br^* + D_2)^2}\right) - \frac{w_2 c^2 (v^* + D_2) v^* r^{*2}}{w_3 k^2 (v^* + br^* + D_2)^2}\frac{\delta_1}{\delta_3} \\
& \qquad < \delta_1\delta_2 k^2 - \frac{w_2 c^2}{w_3 \delta_3 k^4}\frac{(v^* + D_2)}{(v^* + br^* + D_2)^2}\left(-\frac{a_1}{k} + \frac{w_0 v^*}{(u^* + D_0)^2}\right)u^* v^* r^{*2}
\end{aligned} \tag{5.15}$$

$$\left[u^*\left(-\frac{a_1}{k}+\frac{w_0v^*}{(u^*+D_0)^2}\right)(\delta_2+\delta_3)+\frac{w_2r^*(v^*+2(D_2+br^*))}{(v^*+br^*+D_2)^2}(\delta_1+\delta_3)\right]k^2$$
$$-\frac{ww_1D_1u^*v^*}{(u^*+D_0)(u^*+D_1)^2}-\frac{w_2c^2(v^*+D_2)v^*r^{*2}}{w_3(v^*+br^*+D_2)^2}-\frac{w_2(v^*+2(D_2+br^*))u^*r^*}{(v^*+br^*+D_2)^2} \tag{5.16}$$
$$\left(-\frac{a_1}{k}+\frac{w_0v^*}{(u^*+D_0)^2}\right)>(\delta_1\delta_2+\delta_2\delta_3+\delta_3\delta_1)k^4-\frac{det(J_{uvr})}{tr(J_{uvr})}$$

The spatially homogeneous state will be unstable provided that at least one eigenvalue of characteristic equation 5.12 is positive. This will occur when at least one of the three inequalities of *Theorem 5* does not hold.

For the above, since $\delta_1, \delta_2, \delta_3$ and k are all positive, the inequality 5.14 always holds as $a_{11}+a_{22}<0$ from the stability condition of interior point in homogeneous state (Here we will have to refer the analysis of non spatial model). Therefore, the inequality 5.15 can be reversed and can be rewritten as

$$\begin{aligned}H(k^2)=&(k^2)^3\delta_1\delta_2\delta_3-(k^2)^2\left[u^*\left(-\frac{a_1}{k}+\frac{w_0v^*}{(u^*+D_0)^2}\right)\delta_2+\frac{w_2r^*(v^*+2(D_2+br^*))}{(v^*+br^*+D_2)^2}\delta_1\right]\delta_3\\&+k^2\left[\delta_3\left(w_2u^*r^*\left(-\frac{a_1}{k}+\frac{w_0v^*}{(u^*+D_0)^2}\right)\frac{(v^*+2(D_2+br^*)}{(v^*+br^*+D_2)^2}+\frac{w_0w_1D_1u^*v^*}{(u^*+D_0)(u^*+D_1)^2}\right)\right]\\&+k^2\left(\delta_1\frac{w_2c^2}{w_3}\frac{(v^*+D_2)v^*r^{*2}}{(v^*+br^*+D_2)^2}\right)-\frac{w_2c^2}{w_3}\frac{(v^*+D_2)}{(v^*+br^*+D_2)^2}\left(-\frac{a_1}{k}+\frac{w_0v^*}{(u^*+D_0)^2}\right)u^*v^*r^{*2}<0\end{aligned} \tag{5.17}$$

The minimum of $H(k^2)$ occurs at $k^2=k_c^2$ given by

$$\begin{aligned}&\frac{1}{3\delta_1\delta_2\delta_3}\left[\left\{u^*\left(-\frac{a_1}{k}+\frac{w_0v^*}{(u^*+D_0)^2}\right)\delta_2+\frac{w_2r^*(v^*+2(D_2+br^*))}{(v^*+br^*+D_2)^2}\delta_1\right\}\delta_3\right.\\&+\left\{\left\{u^*\left(-\frac{a_1}{k}+\frac{w_0v^*}{(u^*+D_0)^2}\right)\delta_2+\frac{w_2r^*(v^*+2(D_2+br^*))}{(v^*+br^*+D_2)^2}\delta_1\right\}^2\delta_3^2\right.\\&-3\delta_1\delta_2\delta_3\left\{\delta_3\left\{w_2u^*r^*\left(-\frac{a_1}{K}+\frac{w_0v^*}{(u^*+D_0)^2}\right)\frac{v^*+2(D_2+br^*)}{(v^*+br*+D_2)^2}\right\}\right.\\&\left.\left.\left.+\frac{w_0w_1D_1u^*v^*}{(u^*+D_0)(u^*+D_1)^2}\right\}+\delta_1\frac{w_2c^2(v^*+D_2)v^*r^*2)}{w_3(v^*+br^*+D_2)^2}\right\}^{1/2}\right]\end{aligned} \tag{5.18}$$

Consequently, the condition for diffusive instability is $H(k_c^2)<0$.

Theorem 6 The criterion for diffusive instability for the model system is obtained at the critical wave number k_c of the first perturbations obtained by solving 5.18.

6. Turing and Non - Turing Pattern Formation

We now carry out numerical simulations of model system 2.2 and demonstrate the Turing instability. We perform both 1d and 2d simulations. For the simulations we use MATLAB

(R2011a). All the simulations performed have been refined several times on spatial grids in both 1d and 2d. These refinements lead to the same general shape and structure of the figures. All of our calculations are based on perturbations of the non-trivial steady-state. To explore the spatiotemporal dynamics of the model system in two dimensional spatial domain, the system of partial differential equations is numerically solved using a finite difference method. Forward difference scheme is used for the reaction part and standard five point explicit finite difference scheme is used for two dimensional diffusion terms. The model is studied with positive initial condition and Neumann boundary condition in the spatial domain, $0 < x < L_x$, $0 < x < L_y$, where $L_x = L_y = 500$. Parameters used in the simulations are given in Table 1. The initial distribution of the species is considered to be a small spatial perturbation of the steady state. The simulations have been performed for different step sizes in space and time until the solution becomes invariant. To investigate the spatiotemporal dynamics of the model systems, we have numerically solved the system of partial differential equations using finite difference method. Forward difference scheme is used for the reaction part. For diffusion part, central difference scheme is used for one dimensional case and standard five point explicit finite difference technique is used for two dimensional diffusion terms. The simulation is carried out at different time level for both one dimensional and two dimensional spatial model systems.

6.1. Non - Turing pattern formation

We study the model system 3.1 in both one dimension and two dimension. In one dimensional case, the model system with $u(x,t), v(x,t)$ and $r(x,t)$ takes the form as given below

$$\frac{\partial u}{\partial t} = a_1 u\left(1 - \frac{u}{K}\right) - \frac{w_0 uv}{(u + D_0)} + \delta_1 \Delta u \tag{6.1}$$

$$\frac{\partial v}{\partial t} = -a_2 v + \frac{w_1 uv}{u + D_1} - \frac{w_2 vr}{(v + br + D_2)} + \delta_2 \Delta v \tag{6.2}$$

$$\frac{\partial r}{\partial t} = cr^2 - \frac{w_3 r^2}{(v + D_3)} + \delta_3 \Delta r \tag{6.3}$$

The equations 6.1 are solved numerically with zero flux boundary condition at different time levels t =100, 200, 500, 800, and 15000 and results are presented in Fig. 1. The parameter values used for Fig. 1 are as follows:

$$a_1 = 1.93, K = 36, w = 1, D = 10, \delta_1 = 1, a_2 = 1, w_1 = 2, D_1 = 10, w_2 = 0.405$$

$$D_2 = 10, b = 0.2, \delta_2 = 1, c = 0.027, w_3 = 0.8, D_3 = 20, \delta_3 = 1$$

The system of equations 6.1 are numerically solved over 30000 mesh points with very small spatial resolution $Du = 0.1$ and time step $D_t = 0.1$, to avoid any numerical artifact. The nontrivial interior equilibrium for model system 3.1 is $E^{*}(31.6917, 9.6296, 66.8290)$. The initial condition used is of the form δ,

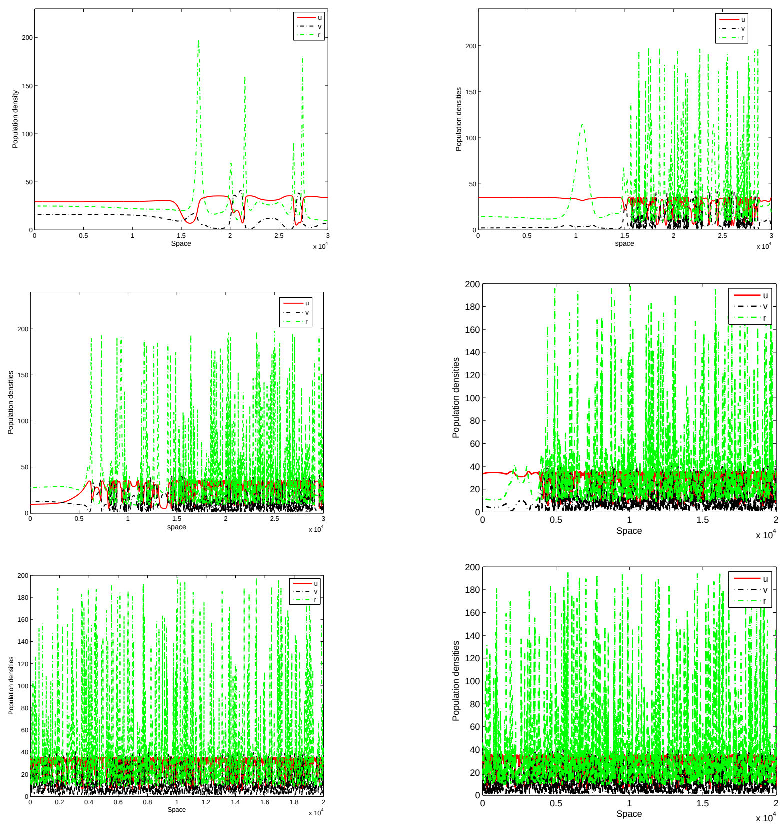

Figure 1: 1 Model System 1: Simulation of model system (24)-(26) at different time level (a) t = 100 (b) t = 200 (c) t = 300 (d) t = 500 (e) t = 800 (f) t = 15000. Parameter values are given in text

$$
\begin{aligned}
u(x,0) &= u^{*} + \epsilon_1 (x-1200)(x-2800) \\
v(x,0) &= v^{*} + \epsilon_2 (x-200)(x-800) \\
r(x,0) &= r^{*}
\end{aligned}
\tag{6.4}
$$

where (u^{*}, v^{*}, r^{*}) is the nontrivial state for the coexistence of the three populations and $\epsilon_1 = \epsilon_2 = 10^{-8}$. At time t =100 , an irregular but less dense dynamics is observed, but as time increases to t = 500 the irregular chaotic patterns increases. The size of the domain occupied by the irregular chaotic patterns increases and hence occupies the whole region at time t = 800 and the chaotic dynamics persists as time increases at t =15000 . At the same set of parameter values given in 3.7, the spatial model system 6.1 displays chaotic attractor shown in Fig. 2.

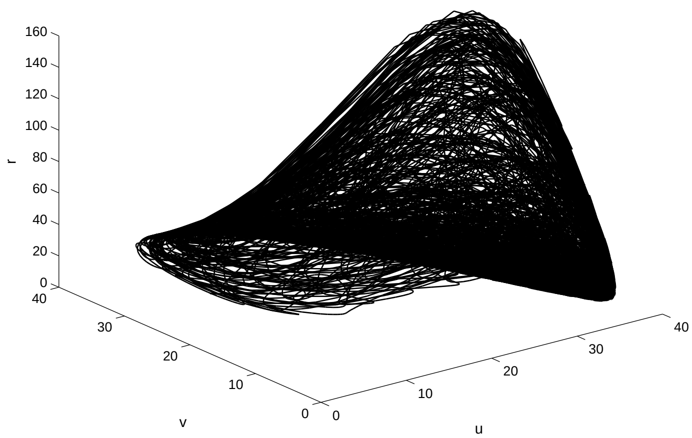

Figure 2: Chaotic attractor obtained due to spatial evolution of trajectories of model system (4)-(6). Parameter values are given in text

The two dimensional spatially extended model system takes the form as given below

$$\frac{\partial u}{\partial t} = a_1 u(1-\frac{u}{K}) - \frac{wuv}{(u+d_0)} + \delta_1 \left(\frac{\partial^2 u}{\partial x^2} + \frac{\partial^2 u}{\partial y^2}\right) \tag{6.5}$$

$$\frac{\partial v}{\partial t} = -a_2 v + \frac{w_1 uv}{u+D_1} - \frac{w_2 vr}{(v+D_2)} + \delta_2 \left(\frac{\partial^2 v}{\partial x^2} + \frac{\partial^2 v}{\partial y^2}\right) \tag{6.6}$$

$$\frac{\partial r}{\partial t} = cr^2 - \frac{w_3 r^2}{(v+D_3)} + \delta_3 \left(\frac{\partial^2 r}{\partial x^2} + \frac{\partial^2 r}{\partial y^2}\right) \tag{6.7}$$

The system of equations 6.5 is numerically solved over a 500×500 square spatial domain with spatial resolution $\Delta u = 1 = \Delta v$ and time step $\Delta t = 0.1$. The spatial patterns of the three populations, u, v, r, are presented in Fig. 3 at different time with other parameter values same as given in 3.7. Note that the initial conditions are deliberately chosen so that it is asymmetrical in order to make more influence of the corners of the domain. The initial distribution of the species considered is a two-dimensional initial condition of the form given below :

$$\begin{aligned} u(x,y,0) &= u^* + \epsilon_1(x - 0.1v - 325)(y - 0.1v - 675) \\ v(x,y,0) &= v^* + \epsilon_2(x - 450) - \epsilon_3(y - 350) \\ r(x,y,0) &= r^* \end{aligned} \tag{6.8}$$

where, (u^*, v^*, r^*) is the nontrivial state for the coexistence of the three species and $\epsilon_1 = 2 \times 10^{-7}, \epsilon_2 = 3 \times 10^{-5}$ and $\epsilon_3 = 1.2 \times 10^{-4}$ The spatial snapshots of three populations at different time levels $t = 500, 800, 1000and1500$ are presented in Fig 3 with initial conditions as specified and other parameter values given in 3.7.

Simulations are performed over the square domain of 1000×1000 with spatial resolution $\Delta x = \Delta y = 0.01$ and time step size 0.01. We next present the results of the 2d simulations in Figures 3. The densities of the three species are shown as contour plots in the $x - y$ plane (see table 1 for the parameters). The long-time pattern is seen to be spot Turing patterns, with cold and hot spots being most conspicuous, in case of the prey and the middle predator respectively.

7. Turing pattern Formation

Long term numerical simulation is carried out for the solution of the model system 2.2. The parameter values are chosen such that the Turing instability conditions derived in section 4 are satisfied. The system is solved under Neumann boundary conditions. The initial condition used is a two dimensional spatial perturbation of the order 10^{-7} and 10^{-5} to the coexistence steady state of the system. The parameter values used are given in table below. For the numerical integration, the time step has been fixed at $\frac{1}{3}$ but we keep changing the space step and the domain size which yield a wide range of Turing patterns as seen in Fig 4 to Fig 10. The different values of diffusivity constants and other parameters used for simulation are presented in Table 1.

Table 1: Table describing different parameters values and corresponding diffusivity coefficients used for simulation.

Fig.	δ_1	δ_2	δ_3	space-step	domain size	time
4	1.25×10^{-3}	1.25×10^{-3}	1.25	2	500 x 500	1500
5	3×10^{-2}	3×10^{-2}	3	3	500 x 500	2000
6	3×10^{-2}	3×10^{-2}	3	3	1000 x 1000	2000
7	3×10^{-2}	3×10^{-2}	3	2	1000 x 1000	5000
8	3×10^{-1}	3×10^{-1}	3	2	1000 x 1000	2000
9	3×10^{-1}	3×10^{-1}	3	2	1000 x 1000	5000
10	3×10^{-3}	3×10^{-3}	3	2	1000 x 1000	5000

8. Hopf-Bifurcation and Pattern Formation

In this section, we perform a detailed bifurcation analysis of the system 2.2. Bifurcation study has been done by selecting the bifurcation parameter as a_1 the rate of self-growth of prey as bifurcation parameter because from the Hopf bifurcation analysis we have observed that a_1 is one of the sensitive parameters, which has a significant impact on the dynamics of the model system 2.2. For bifurcation study, we discretize the model system 2.2 in space. In this section,

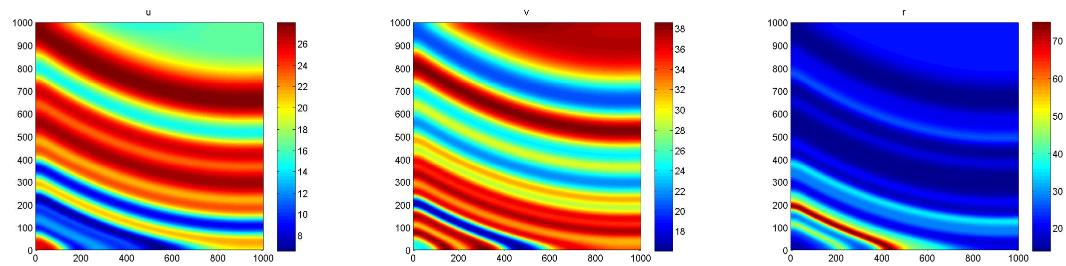

(a)

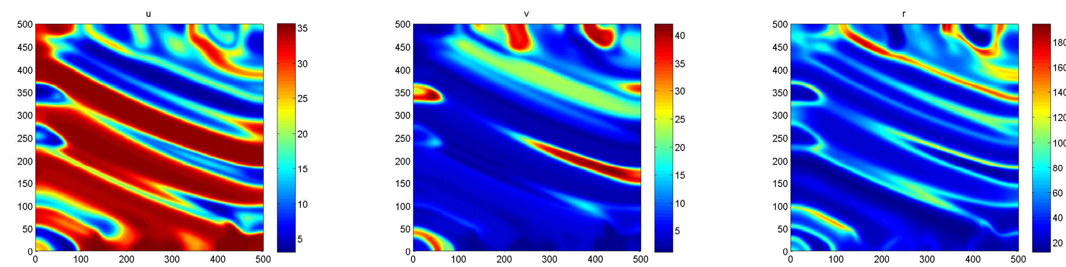

(b)

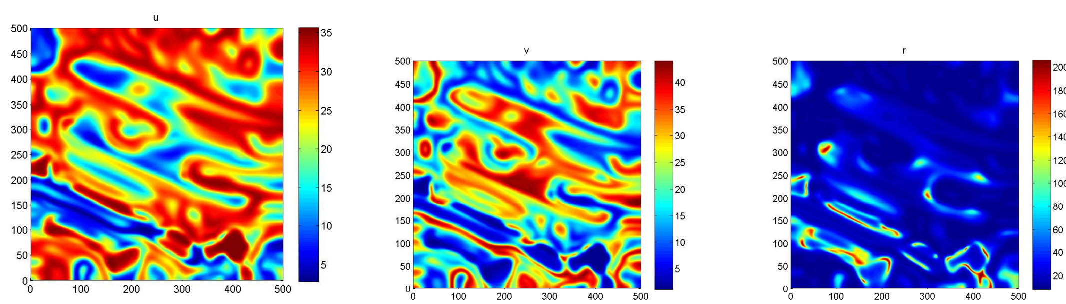

(c)

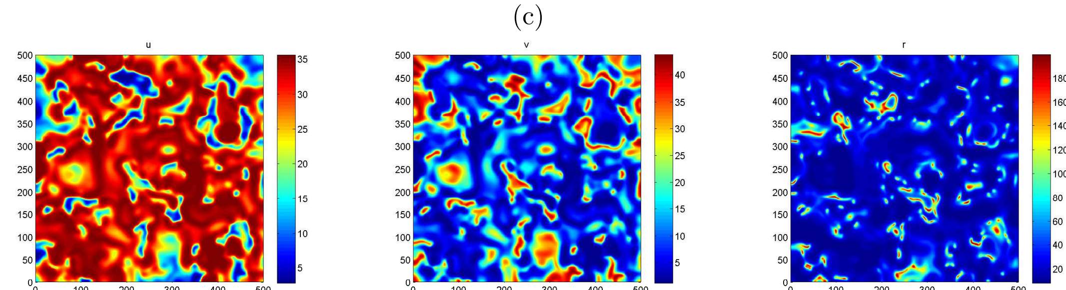

(d)

Figure 3: Spatial snapshots are obtained at different time a) t = 500 b) t = 800 c) t = 1000 d) t =1500. Parameter values are same as in one dimensional case with initial condition give in (18). Other parameter values are in text.

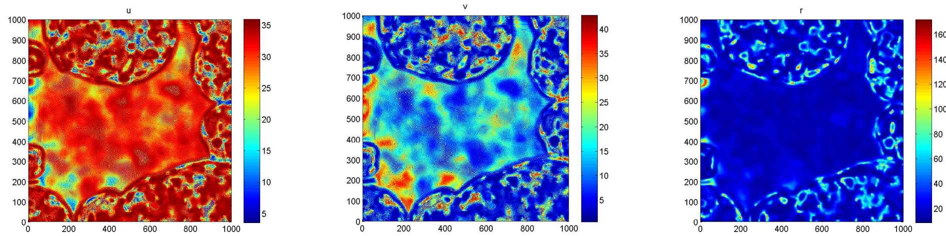

Figure 4: Solutions of the model system (4)-(6) showing Turing patterns. Here the domain size is increased and step size is reduced relative to Fig 5 and other parameters are kept constant

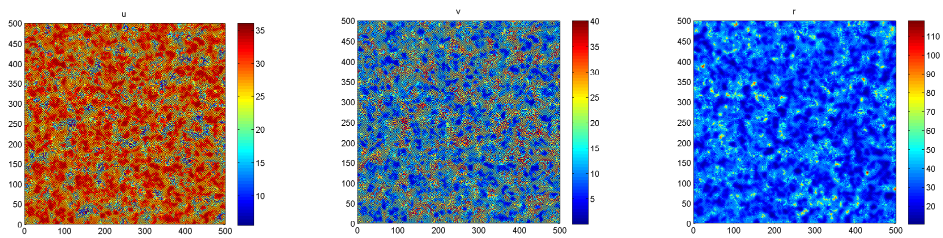

Figure 5: Solutions of the model system (4)-(6) showing sprinkle type Turing patterns at t=1500. First second and third figure represents prey, middle predator and top predator population distributions respectively.

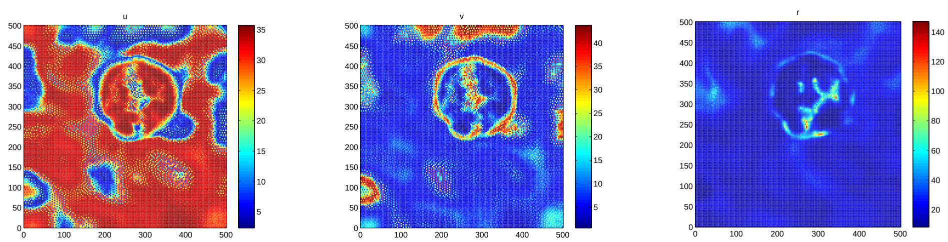

Figure 6: Solutions of the model system (4)-(6) showing Turing patterns where prey population displays a circular patch of high population density and middle predator yields a circular ring of high population density . We here increase the diffusion coefficients of all three populations.

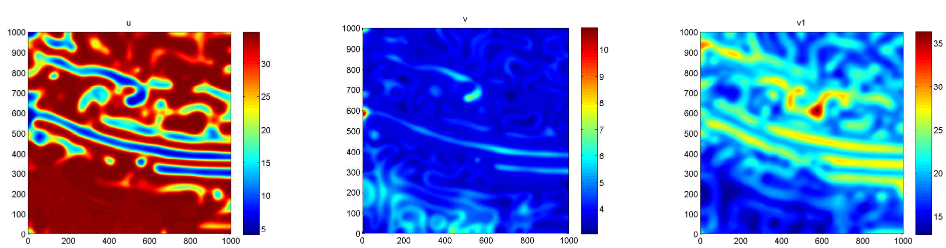

Figure 7: Solutions of the model system (4)-(6) showing Turing patterns. Here we increase the value of diffusion coefficients of the prey and the middle predator and keep the diffusion coefficient of the top predator fixed

the discretized system of dimension 10 of the reaction diffusion system is used for simulation.We have plotted bifurcation diagram with respect to a_1.

We have considered all the diffusivity coefficients of prey, mid predator and top predator to be

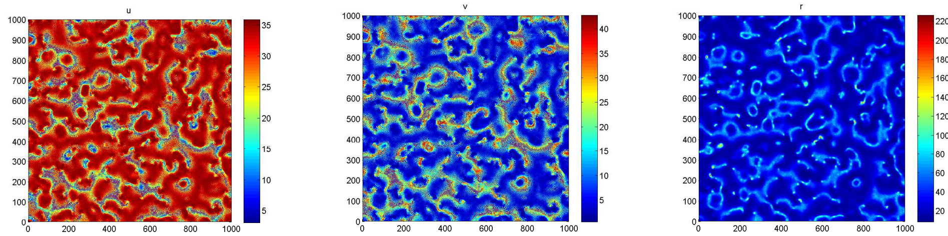

Figure 8: Solutions of the model system (4)-(6) showing Turing patterns when numerical integration is carried for relatively longer time 5000

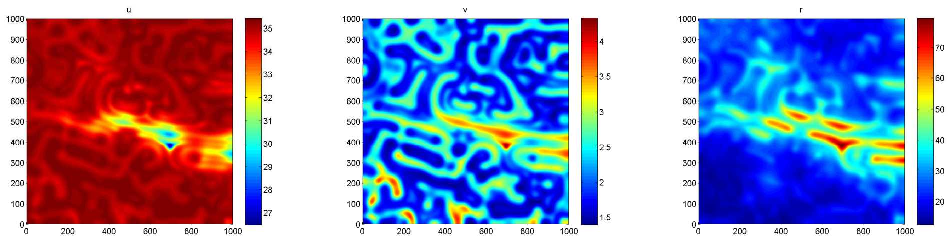

Figure 9: Solutions of the model showing Turing patterns when numerical integraion is done for longer time while other parameters remain fixed as in Fig 8.

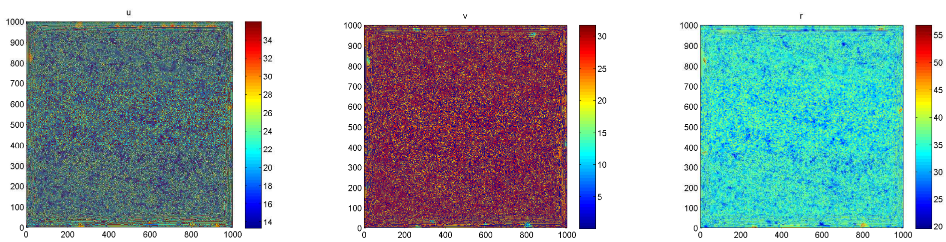

Figure 10: Solutions of the model showing Turing patterns. Here we reduce the diffusion coefficients of prey and predator population significantly while keeping the diffusion coefficient of top predator fixed.

equal or same therefore, $D = \delta_1 = \delta_2 = \delta_3$. Since, diffusion coefficient is a responsible parameter for pattern formation. We study the change variation in dynamics with respect to D, the equal diffusivity coefficient. So we change the value of D as $D = 10, 30, 50,$ and 70 and we plot bifurcation diagram in Fig 11(a).

We observed that for the smaller values of $D = 10, 30,$ and 50 the dynamics is very complex and displays several Hopf Bifurcation points, the system displays fewer number of Hopf Bifurcation points at $D = 70$.

Further in Fig-11(b), we perform the bifurcation study at $D = 100, 400, 500, 600, 800$.

Here we observe that the number of Hopf Bifurcation points becomes constant and its value converges to $'3'$.

At equal diffusivity coefficient $\delta_1 = \delta_2 = \delta_3 = 800$, the Hopf-bifurcation points are obtained at the bifurcation parameter value $a_1 = 0.860982, 0.730893$ and 0.702050 and a limit point is obtained at 0.655325. In fig 12a, we obtain spatial distribution of prey density at $a_1 = 0.68$ which is the point before Hopf-bifurcation point $a_1 = 0.70205$. The prey distribution is almost homogeneous in space at this point.

We further simulate pattern at $a_1 = 0.71$ the value of bifurcation parameter between the two Hopf bifurcation points $0.70205 and 0.730893$(see fig 12b).Again we observe a homogeneous population density distribution in space. The spatial distribution obtained at $a_1 = 0.75$ and $a_1 = 1.93$ is presented in fig 12c and 12d respectively. The numerical integration is done at time 1500 for fig 12. We observe a homogeneous prey population distribution at all values of bifurcation parameter a_1 which are less than 0.86. When the value of a_1 is larger than 0.86, which is Hopf bifurcation point, we obtain a complex spatial distribution (see Fig 12d).

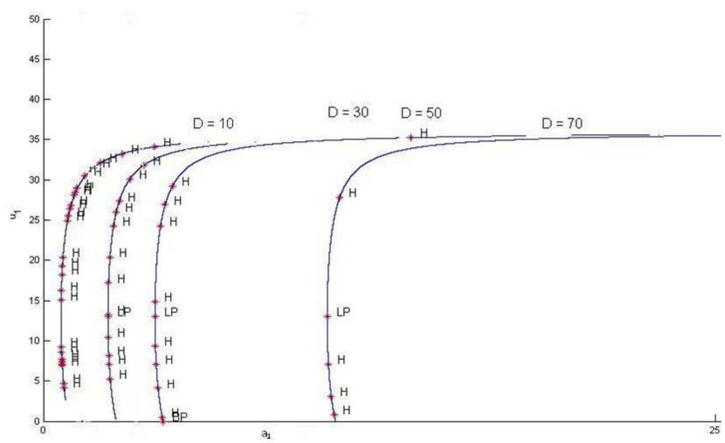

(a)

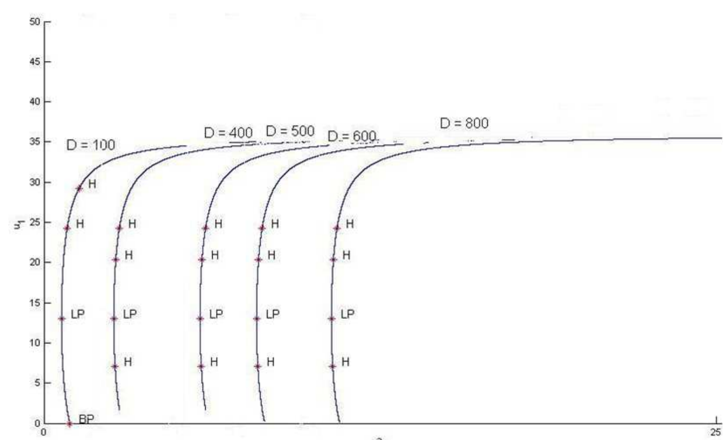

(b)

Figure 11: The bifurcation diagram at diffusivity coefficients (a) D= 10,30,50,70 (b) D= 100,400,500,600,800

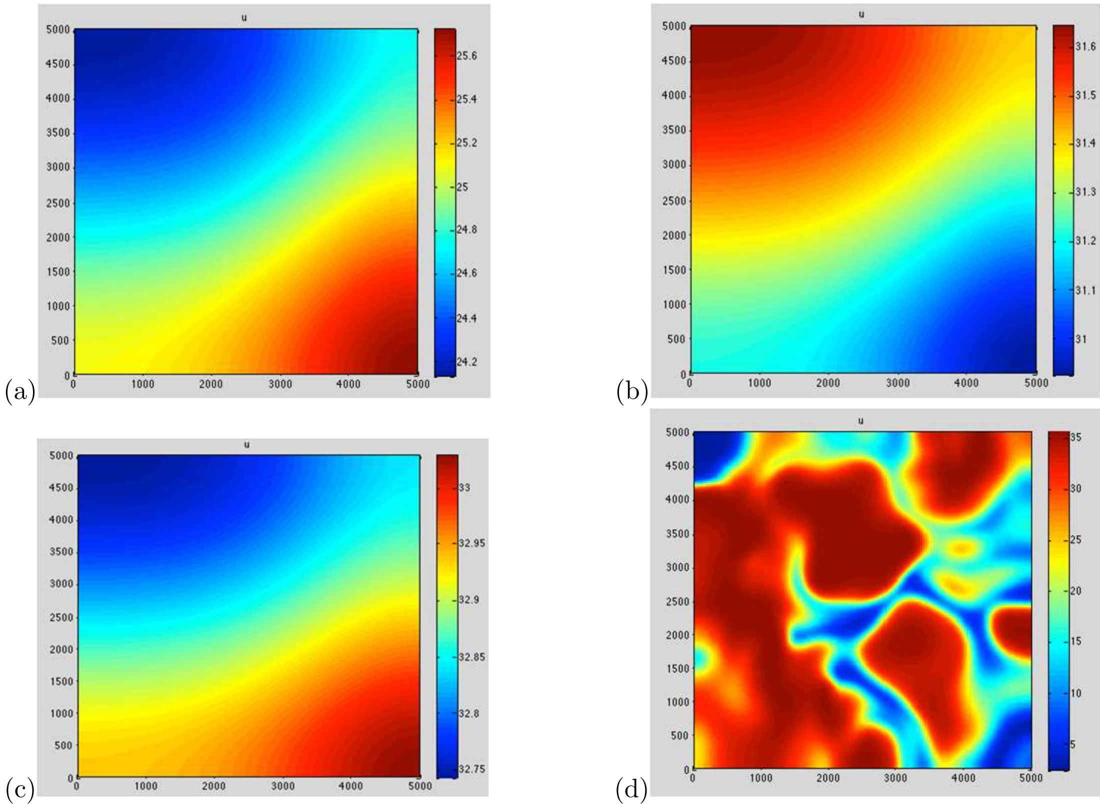

Figure 12: Patterns obtained at different values of bifurcation parameter a_1 (a) $a_1 = 0.68$, space step = 20 (b) $a_1 = 0.71$ space step = 20 (c) $a_1 = 0.75$, space step = 20 (d) $a_1 = 1.93$, space step = 30

9. Discussion and conclusion

In this work, we have analytically and numerically investigated three species diffusive interaction model of hyperparasitoid, parasitoid and host population with Beddington DeAngelis functional response. An extensive stability analysis of the temporal system and spatially extended model system has been carried out which includes both local and global stability analysis at various equilibrium points in concern. Moreover, it has been proved that the Beddington DeAngelis functional response admits a wide range of dynamical behaviour including Hopf bifurcation, limit points, Turing and non Turing patterns.

The existence of Hopf bifurcation has been shown both analytically and numerically with respect to parameter a_1 - which is the rate of self growth of prey because it is a sensitive parameter and it governs the dynamics both middle order predator and top level predator significantly and in turn the dynamics of the system. The bifurcation diagram at different values of diffusivity constants is obtained (Fig 11) which shows different Hopf bifurcation points for different values of bifurcation parameter a_1 and also corresponding limit points.

The one dimensional model system has been solved numerically with zero flux conditions at different time levels and results are depicted in Fig-1 at different parameter values, also it has been shown in Fig-2 that the model system displays chaotic attractor.Extensive study of two dimensional spatially extended model system has been carried out. Various spatial snapshots at different time levels are given in Fig-3. The conditions for the occurrence of diffusion driven instability has been derived and numerical simulations of the system has been carried out to demonstrate Turing instability Simulations have been performed for parameters which satisfy the conditions derived for Turing instability. For different domain size, step size and diffusion coefficients values of species involved, Turing patterns have appeared in the system which are depicted in Fig - 4, 5,6, 7, 8, 9 and 10. The relationship between Hopf bifurcation and Turing pattern formation has been shown in Fig - 12(a), 12(b), 12(c) and 12(d).

The mutual interference in the model yields an oscillatory spatiotemporal growth to the middle predator in a three species model. In Fig 3(a) the spatial distribution of middle predator is high at various locations. At time t=800, the population density of v decreases significantly (Fig 3(b)). But again there is significant population growth at various locations at t = 1000 followed by population decline at t = 1500 (Fig3c-d). However, the spatiotemporal pattern formation of top predator population r, who predates on the middle predator using Beddington DeAngelis functional response, exhibits a continuous decline in the population density. This shows that Beddington DeAngelis predator response provides an advantage to the middle predator v to grow over time when the population is spatially distributed and simultaneously restricts the bloom in the population.

9.1. Acknowledgments

The work of the corresponding author (NK) was supported by Science Engineering Research Board (SERB) India under three separate grants with grant numbers MTR/2018/000727, EMR/2017/005203 and MSC/20202/000369.

References

[1] Alan Mathison Turing. The chemical basis of morphogenesis. *Bulletin of mathematical biology*, 52(1):153–197, 1990.

[2] Wei-Ming Ni and Izumi Takagi. On the neumann problem for some semilinear elliptic equations and systems of activator-inhibitor type. *Transactions of the american Mathematical society*, 297(1):351–368, 1986.

[3] Mingxin Wang. Non-constant positive steady states of the sel'kov model. *Journal of Differential Equations*, 190(2):600–620, 2003.

[4] Rui Peng and Mingxin Wang. Positive steady-state solutions of the noyes–field model for belousov–zhabotinskii reaction. *Nonlinear Analysis: Theory, Methods & Applications*, 56(3):451–464, 2004.

[5] Juncheng Wei and Matthias Winter. Existence and stability of multiple-spot solutions for the gray–scott model in¡ i¿ r¡/i¿¡ sup¿ 2¡/sup¿. *Physica D: Nonlinear Phenomena*, 176(3):147–180, 2003.

[6] Wei-Ming Ni and Juncheng Wei. On positive solutions concentrating on spheres for the gierer–meinhardt system. *Journal of Differential Equations*, 221(1):158–189, 2006.

[7] Shigeru Kondo. The reaction-diffusion system: a mechanism for autonomous pattern formation in the animal skin. *Genes to Cells*, 7(6):535–541, 2002.

[8] John L Maron and Susan Harrison. Spatial pattern formation in an insect host-parasitoid system. *Science*, 278(5343):1619–1621, 1997.

[9] Shigeru Kondo and Takashi Miura. Reaction-diffusion model as a framework for understanding biological pattern formation. *Science*, 329(5999):1616–1620, 2010.

[10] Chris Cosner, Donald L DeAngelis, Jerald S Ault, and Donald B Olson. Effects of spatial grouping on the functional response of predators. *Theoretical Population Biology*, 56(1):65–75, 1999.

[11] Robert Stephen Cantrell and Chris Cosner. On the dynamics of predator–prey models with the beddington–deangelis functional response. *Journal of Mathematical Analysis and Applications*, 257(1):206–222, 2001.

[12] Mainul Haque. Existence of complex patterns in the beddington–deangelis predator–prey model. *Mathematical biosciences*, 239(2):179–190, 2012.

[13] Wei Han and Zhenhua Bao. Hopf bifurcation analysis of a reaction–diffusion sel'kov system. *Journal of Mathematical Analysis and Applications*, 356(2):633–641, 2009.

[14] Jia-Fang Zhang, Wan-Tong Li, and Xiang-Ping Yan. Hopf bifurcation and turing instability in spatial homogeneous and inhomogeneous predator–prey models. *Applied Mathematics and Computation*, 218(5):1883–1893, 2011.

[15] Zhan-Ping Ma, Wan-Tong Li, and Xiang-Ping Yan. Stability and hopf bifurcation for a three-species food chain model with time delay and spatial diffusion. *Applied Mathematics and Computation*, 2012.

[16] Xiaoling Zou, KE Wang, and Dejun Fan. Stochastic poincaré–bendixson theorem and its application on stochastic hopf bifurcation. *International Journal of Bifurcation and Chaos*, 23(04), 2013.

[17] Ranjit Kumar Upadhyay, SRK Iyengar, and Vikas Rai. Chaos: an ecological reality? *International Journal of Bifurcation and Chaos*, 8(06):1325–1333, 1998.

[18] Ranjit Kumar Upadhyay and Vikas Rai. Why chaos is rarely observed in natural populations. *Chaos, Solitons & Fractals*, 8(12):1933–1939, 1997.

[19] RK Upadhyay, RK Naji, and N Kumari. Dynamical complexity in some ecological models: effect of toxin production by phytoplankton. *Nonlinear Analysis: Modelling and Control*, 12(1):123–138, 2007.

[20] RK Upadhyay and J Chattopadhyay. Chaos to order: role of toxin producing phytoplankton in aquatic system. *Nonlinear Analysis: Modelling and Control*, 10(4):383–396, 2005.

[21] Nitu Kumari. Pattern formation in spatially extended tritrophic food chain model systems: generalist versus specialist top predator. *ISRN Biomathematics*, 2013, 2013.

[22] Garrick T Skalski and James F Gilliam. Functional responses with predator interference: viable alternatives to the holling type ii model. *Ecology*, 82(11):3083–3092, 2001.